

# Multiscale Modeling of Laser Ablation: Applications to Nanotechnology

Leonid V. Zhigilei<sup>1</sup> and Avinash M. Dongare<sup>1</sup>

**Abstract:** Computational modeling has a potential of making an important contribution to the advancement of laser-driven methods in nanotechnology. In this paper we discuss two computational schemes developed for simulation of laser coupling to organic materials and metals and present a multiscale model for laser ablation and cluster deposition of nanostructured materials. In the multiscale model the initial stage of laser ablation is reproduced by the classical molecular dynamics (MD) method. For organic materials, the breathing sphere model is used to simulate the primary laser excitations and the vibrational relaxation of excited molecules. For metals, the two temperature model coupled to the atomistic MD model provides an adequate description of the laser energy absorption into the electronic system and fast electron heat conduction. A combined MD - finite element method and the dynamic boundary condition are used to avoid reflection of the laser-induced pressure wave from the boundary of the MD computational cell. The direct simulation Monte Carlo method is used for simulation of the long term ablation plume expansion, and the MD method is used to simulate film growth by cluster deposition from the ablation plume. The proposed multiscale approach is applied to investigate the mechanisms of cluster formation in laser ablation and to analyze the distributions of clusters of different sizes in the ejected plume. MD simulations of cluster deposition are performed for different impact velocities and a strong dependence of the structure of the growing films on the parameters of the deposited clusters is revealed. A new technique for controlled implantation of functional organic molecules into sub-micron regions of a polymer substrate is investigated in molecular-level simulations and different regimes of molecular transfer are discussed.

## 1 Introduction

Irradiation of a solid or liquid target with a laser pulse of a sufficiently high intensity can lead to the massive material removal from the target. This phenomenon, called laser ablation, is used in a wide range of well-established applications, from laser surgery [e. g. Niemz 1996] and laser-driven mass-spectrometry of biomolecules [Hiltenkamp and Karas 2000] to surface microfabrication and pulsed laser deposition (PLD) of films and coatings [Chrissey and Hubler 1994; Bäuerle 2000]. Recently, applications of laser ablation have been extended into emerging area of nanotechnology. In particular, laser ablation has been successfully applied for synthesis of fullerenes, carbon nanotubes [Poretzky et al. 1999], and Si nanowires [Zhang et al. 1998], machining of nanostructures with resolutions exceeding the optical diffraction limit [Jersch et al. 1997], generation of nanoparticles and deposition of nanocrystalline or cluster-assembled materials [Chrissey and Hubler 1994; Fitz-Gerald et al. 1999; Bäuerle 2000; Ayyub et al. 2001]. Further optimization of experimental parameters in current applications and design of new laser processing and fabrication techniques for nanotechnology can be facilitated by a better theoretical understanding of the relations between the basic mechanisms of laser interaction with materials, non-equilibrium processes caused by the fast deposition of laser energy, and the resulting microstructure and properties of the materials treated by laser irradiation or produced by the ablation plume deposition.

Theoretical and computational investigation of the laser ablation phenomenon is challenging due to the complex collective character of the involved processes that occur at different time and length scales. The processes include primary elementary excitations of optically active states in a solid, thermalization of the deposited laser energy, formation of a highly energetic high-temperature and high-pressure region, explosive disintegration and prompt forward ejection of a volume of material, intensive processes in the ejected plume, propagation of a

---

<sup>1</sup>Department of Materials Science & Engineering, University of Virginia; 116 Engineer's Way, Charlottesville, Virginia 22904

pressure wave to the bulk of the target away from the ablation region, etc. It is impossible to address all the diverse and intertwined processes within a single computational model. In order to address different processes involved in laser ablation with appropriate resolutions and, at the same time, to account for the interrelations between the processes, a computational approach that combines different methods within a single multiscale model should be developed. A general description of the elements of the multiscale model for laser ablation and deposition of nanostructured materials is presented next, in Section 2. Some of the results from computational investigation of the mechanisms of nanoparticles formation in laser ablation are presented in Section 3. Simulations aimed at understanding of different regimes of molecular transfer in a new technique for controlled implantation of functional organic molecules into designated sub-micron regions of a polymer substrate [Goto et al. 1999, 2000] are discussed in Section 4.

## 2 Multiscale model for laser ablation

The hierarchy of computational methods used to simulate different processes involved in laser ablation and film growth by cluster deposition from the ablation plume is schematically illustrated in Figure 1. We start the discussion of the multiscale model from Part A that represents molecular dynamics (MD) modeling of the active processes in the irradiated target leading to the material ejection (ablation). Depending on the irradiation conditions, these processes include melting and hydrodynamic motion of the liquid layer, explosive boiling, or photomechanical spallation [e.g. Oraevsky et al. 1995; Itzkan 1995; Miotello 1999; Zhigilei and Garrison 2000; Zhigilei 2002]. Primary laser excitation mechanisms as well as characteristic times and channels of the relaxation/thermalization of the absorbed laser energy depend on the type of material and the laser parameters. Thus, system-specific computational approaches should be developed for incorporation of the description of the interaction of laser light with target material into the classical MD technique. Below we briefly outline two computational schemes developed for simulation of laser coupling to organic materials and metals.

### 2.1 Organic materials: the breathing sphere model

A collective character of laser ablation occurring at the mesoscopic rather than atomic/molecular scale does not

permit a direct application of the atomistic simulation approach. In an atomistic MD model of an organic system a typical small molecule or a monomer unit can include tens of atoms and the time-step of integration of the equations of motion as small as  $\sim 0.1$  fs must be used to follow high-frequency vibrational motion of H, C, and N atoms. In order to overcome the limitations of the atomistic MD model and to address collective processes leading to material ejection in laser ablation, an alternative coarse-grained "breathing sphere" MD model has been developed [Zhigilei et al. 1997, 1998]. The breathing sphere model assumes that each molecule (or appropriate group of atoms) can be represented by a single particle that has the true translational degrees of freedom but an approximate internal degree of freedom. The internal degree of freedom is attributed to each molecule by allowing the particles to change their sizes. The characteristic frequency of the internal motion is controlled by the parameters of an anharmonic potential. The rate of the intermode energy transfer is determined by the size of the anharmonicity and frequency mismatch between vibrational modes. Thus, the parameters of the internal potential can be used to affect the coupling between the internal and translational molecular motions and to achieve a desired rate of the conversion of internal energy of the molecules excited by the laser to the translational and internal motion of the other molecules. The rate of the vibrational relaxation of excited molecules is an input parameter in the model and can be either measured in ultrafast pump-probe experiments [e.g. Deák et al. 2000] or calculated in atomistic or *ab initio* MD simulations [e.g. Kim and Dlott 1991].

The effect of laser irradiation is simulated by vibrational excitation of molecules randomly chosen within the laser penetration depth appropriate for a given wavelength. The molecules are being excited during the laser pulse and each vibrational excitation is modeled by depositing a quantum of energy equal to the photon energy into the kinetic energy of internal vibration of a given molecule. The absorption probability can be modulated by Beer's law to reproduce the exponential attenuation of the laser light with depth or can be restricted to a certain component within a complex material. In molecular systems a vibrational excitation can occur with infrared (IR) irradiation, when resonant absorption into OH or NH stretching vibrations determines the laser light absorption of a material, and with ultraviolet (UV) irradiation, when

electronic excitations of molecular chromophores (typically a pyridine ring or an other aromatic  $\pi$ -electron system in a matrix molecule) relax by internal conversion to the vibrational excitations of a molecule. An alternative result of UV photon absorption is photofragmentation, when an excited molecule reacts photochemically and forms fragments. The resulting molecules typically occupy a larger volume and create pressure inside the irradiated volume which can then convert to translational energy of ablation. Photochemical processes have been recently incorporated into the breathing sphere model and first simulations, in which an excited molecule can break into radicals and subsequently undergoes abstraction and recombination reactions, have been performed [Yingling et al. 2001].

Because the molecules and not the atoms are the particles of interest in the breathing sphere model, the system size can be significantly larger. Moreover, since explicit atomic vibrations are not followed, the time-step in the numerical integration is longer. Simulations performed with the breathing sphere model have shown that both time- and length-scales of the model can be large enough to reproduce the collective dynamics leading to laser ablation and damage [e.g. Zhigilei et al. 1997, 1998; Zhigilei and Garrison 2000; Yingling et al. 2001; Zhidkov et al. 2001; Zhigilei 2002]. One more advantage of the breathing sphere model is the ability to simulate complex multicomponent organic materials. One can easily include bonding interactions [Itina 2002], different strengths and absorptions of different components [Williams et al. 2001; Zhigilei and Garrison 1998]. The rate of energy transfer within an individual component as well as between components can be precisely controlled.

## 2.2 Laser ablation of metals: heat conduction by free electrons and electron-phonon coupling

In metals, laser light is absorbed by the conduction band electrons. The deposited energy quickly, within femtoseconds, is equilibrated among the electrons and, more slowly, is transferred to the lattice vibrations. The later process is controlled by the strength of the electron-phonon coupling and can take from fraction of a picosecond to several tens of picoseconds. Finally, a thermal equilibrium is established between the electrons and phonons, and the common thermal diffusion can be used to describe the heat flow into the bulk of the irradiated target.

Several modifications have to be made in order to apply the classical MD method for simulation of laser ablation of metals. First, since electronic contribution to the thermal conductivity of a metal is dominant, the conventional MD method, where only lattice contribution is present, significantly underestimates the total thermal conductivity. This leads to unphysical confinement of the deposited laser energy in the surface region of the irradiated target and does not allow for the direct comparison between the calculated and experimental data. This problem has been recognized in first simulations of laser ablation of metals by Ohmura and Fukumoto (1996) and a modified method, in which the MD computational cell is divided into small blocks and Fourier law is applied between the adjacent blocks to account for the heat conduction by free electrons, is proposed [Ohmura and Fukumoto 1997].

From the physical point of view, application of the Fourier law or the equation of heat conduction in metals implies that a complete local thermal equilibrium is reached between the electrons and phonons. This assumption is correct as soon as the duration of the laser pulse is much longer than the characteristic time of electron-phonon relaxation. For ps- and fs-pulses, however, the electron-phonon equilibrium cannot be assumed *a priori* and the time evolution of the lattice and electron temperatures,  $T_l$  and  $T_e$ , can be described by two coupled non-linear differential equations [Anisimov et al. 1974]:

$$C_e(T_e) \frac{\partial T_e}{\partial t} = \nabla(K_e \nabla T_e) - G(T_e - T_l) + S(z, t)$$

$$C_l(T_l) \frac{\partial T_l}{\partial t} = \nabla(K_l \nabla T_l) + G(T_e - T_l)$$

where  $C$  and  $K$  are the heat capacities and thermal conductivities of the electrons and lattice as denoted by subscripts  $e$  and  $l$ , and  $G$  is the electron-phonon coupling constant. The source term  $S(z, t)$  is used to describe the local laser energy deposition per unit area and unit time during the laser pulse duration. The two-temperature model can be incorporated into the classical MD technique by adding an additional coupling term into the MD equations of motion [Häkkinen et al. 1993; Schäfer et al. 2002b; Ivanov and Zhigilei 2002]. In this computational scheme, the diffusion equations are solved simultaneously with MD integration and the electron temperature enters the coupling term that is responsible for the

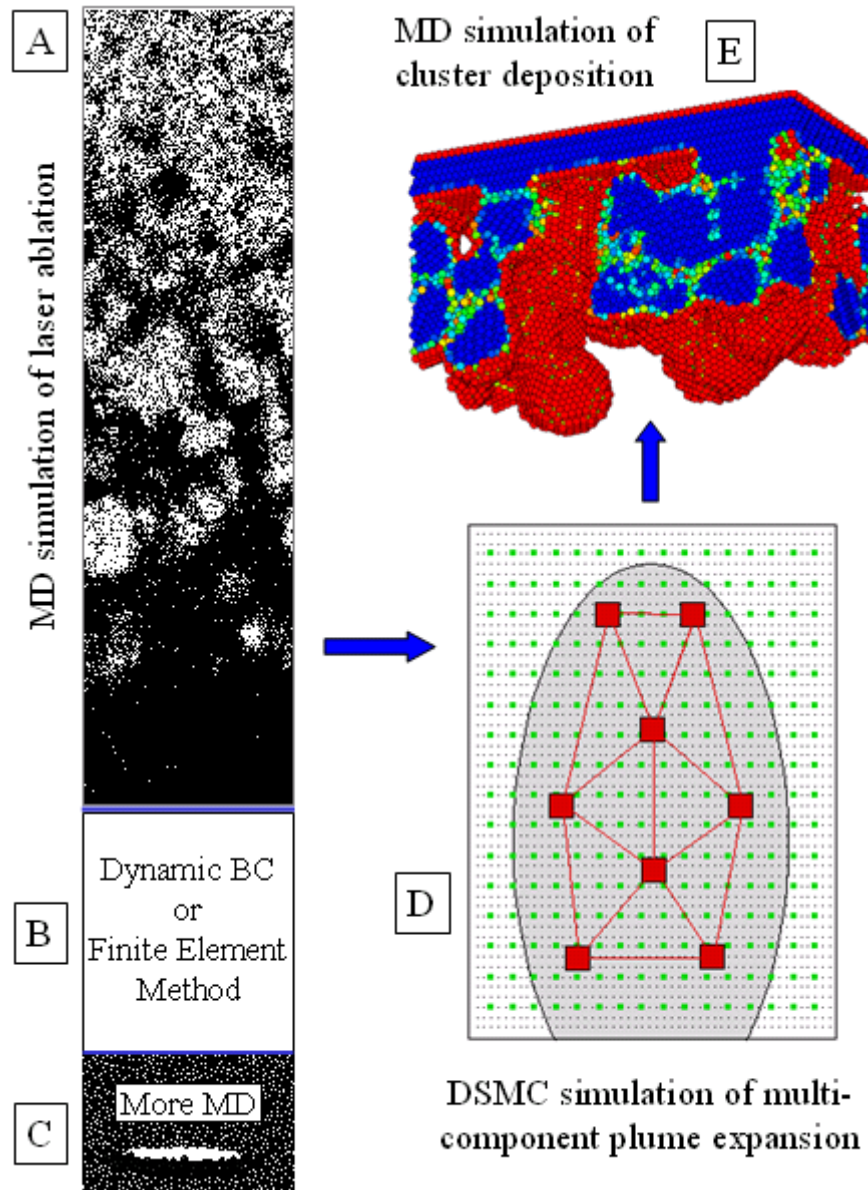


**Figure 1** : Schematic representation of the hierarchy of computational methods that can be used to study formation of clusters in laser ablation and film growth by cluster deposition (see explanation in the text).

energy exchange between the electrons and the lattice. The MD method is used only in the very surface region of the target, where active processes of laser melting and ablation are taking place, Part A in Figure 1, whereas the diffusion equations are solved in a much wider region affected by the thermal conduction from the absorbing surface layer, Part B in Figure 1. Inter-atomic interaction in the MD part can be described by the embedded-atom method [Daw et al. 1993], which provides a computationally efficient but rather realistic description of bonding in metals and allows for simulation of sufficiently large systems. The hybrid approach, briefly described above, combines the advantages of the two-temperature model and the MD method. The two-temperature model provides an adequate description of the laser energy absorption into the electronic system, energy exchange between the electrons and phonons, and fast electron heat conduction in metals, whereas the MD method is appropriate for simulation of non-equilibrium processes of lattice superheating, melting, and ablation.

For simulation of laser ablation of semiconductors, a computational approach that includes a description of the relaxation of a dense gas of hot electrons and holes generated by the laser pulse into the classical MD model is being developed by Lorazo et al. (2000).

### 2.3 Computational methods for non-reflecting propagation of the laser-induced pressure waves

The generation of stress waves is a natural result of the fast energy deposition in the case of short pulse laser irradiation. For example, the formation and propagation of a plane pressure wave in a simulation of laser ablation of an organic target irradiated with a 15 ps laser pulse [Zhigilei and Garrison 2000] is shown in the form of the pressure contour plots in Figure 2. In this case the high compressive pressure builds up in the surface region of the irradiated target due to the thermoelastic stresses and ablation recoil and drives a strong compression wave into the bulk of the sample. Simulation of the propagation of the pressure wave requires the size of the MD computational cell to be increased linearly with the time of the simulation. For times longer than a hundred of picoseconds the size of the model required to follow the wave propagation becomes computationally prohibitive. If large computational cells are not used, however, artificial border effects can interfere with the simulation results. Both rigid and free boundary conditions lead to the complete reflection

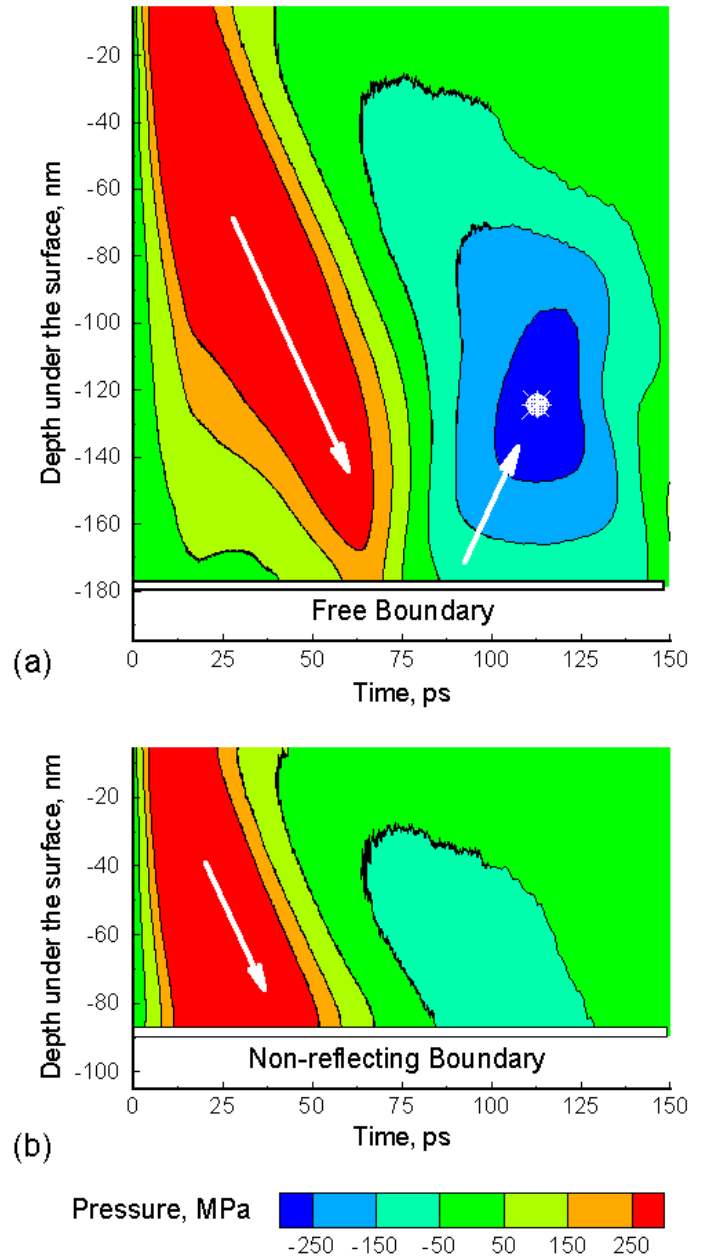


**Figure 2** : Pressure contour plot for MD simulations of 15 ps laser pulse irradiation of an organic target performed with (a) free boundary condition and (b) the dynamic nonreflecting boundary condition at the bottom of the MD cell.

of the pressure wave. The reflection from the free boundary is illustrated in Figure 2a. The compressive pressure wave transforms into the tensile one upon reflection and can cause the effect known as back spallation [e.g. Dekel et al. 1998], when the tensile strength of the material is exceeded by the reflected (tensile) pressure wave and fracturing occurs at a certain depth near the back surface of the sample. The depth and time of the back spallation is marked in Figure 2a and the microscopic picture of the spallation process is shown in Part C of Figure 1. The reflected wave can also reach the front surface of the irradiated sample and contribute to the material ejection.

In order to avoid artifacts due to the pressure wave reflection, a simple and computationally efficient boundary condition based on analytical evaluation of forces acting at the molecules in the boundary region from the outer "infinite medium" has been developed [Zhigilei and Garrison 1999]. In this approach the boundary condition is a set of terminating forces that are applied to the molecules in the boundary region. In the calculation of the terminating forces, that are updated at each integration timestep, three effects are taken into account, namely, the static forces that mimic interaction with molecules beyond the computational cell, the forces due to the direct laser energy absorption in and around the boundary region during the laser pulse, and the forces due to the pressure wave propagation through the boundary region. The contribution of the pressure wave to the terminating forces is calculated based on the traveling wave equation and is proportional to the instantaneous velocity of the boundary.

As shown in Figure 2b, the dynamic boundary condition allows one to simulate non-reflective propagation of the pressure wave through the boundary of the MD computational cell and to restrict area of the MD simulation to the region where active processes of laser induced melting, ablation and damage occur. Although a rather small computational cell is used in the simulation performed with the non-reflecting boundary condition, Figure 2b, no artifacts due to the pressure wave reflection are observed. The non-reflecting boundary conditions have been successfully used in simulations of laser ablation and damage of organic materials in which both planar [e.g. Zhigilei and Garrison 2000; Yingling et al. 2001; Zhidkov et al. 2001; Zhigilei 2002] and spherical [Zhigilei and Garrison 1998] pressure waves were generated. Recently the boundary conditions have been im-

plemented and tested for metals [Schäfer et al. 2002a]. An alternative approach to the problem of pressure wave reflection is to combine the MD model with the continuum finite element method [Smirnova et al. 1999; Rudd and Broughton 2000], Part B of Figure 1. The advantage of this approach is the ability to study the long-range propagation of the waves and their interaction with other MD regions of a large system. One possible effect of such interaction is back spallation, discussed above and schematically illustrated in part C of Figure 1.

#### 2.4 Long-term plume expansion: the direct simulation Monte Carlo method

The ablation plume development in a MD simulation, Part A of Figure 1, can be followed up to a few nanoseconds only, whereas the real time-scales of plume expansion in applications such as PLD are in the range of microseconds. In addition to the long time-scales, the length-scale of the simulation should be increased to include an adequate description of the expansion of material ejected from the whole laser spot. While the expansion of the ablation plume in the lateral directions can be neglected during the first nanoseconds, and the periodic boundary conditions are appropriate for MD simulations, both lateral and axial expansion of the plume should be taken into account in simulations of the long-term plume development. For a laser spot of 10 – 100  $\mu\text{m}$  and ablation depth of 10 – 100 nm, one can estimate that either for a molecular solid or a metal target the number of atoms/molecules ejected in a single laser shot is in the range from tens of billions to trillions. These numbers are much beyond the limits of the MD simulation technique.

Among several alternative methods that can be considered for simulation of the long-term ablation plume expansion, Part D in Figure 1, the direct simulation Monte Carlo (DSMC) method appears to be the most suitable technique for neutral or weakly ionized ablation plumes. The continuum description, based on the finite element solution of the Navier-Stokes equations, is well suited for high-density collision-dominated flows but is not appropriate for the low densities realized in the rapidly expanding ablation plumes. Moreover, the DSMC has an advantage of providing direct information on the velocity, energy and angular distributions of the involved species, whereas the continuum approach requires the distribution functions as input. Traditional particle-in-cell (PIC) codes only treat ions and electrons; there is no chem-

istry or collisions, although collisions can be included by merging PIC with Monte Carlo collision calculations [Birdsall 1991] or by using the Langevin equation to calculate the Coulomb collision term [Zhidkov and Sasaki 1998; Zhidkov et al. 2001]. The PIC method assumes that particles do not interact with each other directly, but through the fields which they produce according to the Maxwell's equations. In any formulation, the PIC model is not appropriate for treating weakly ionized gases with significant interactions between the ions and neutrals.

The DSMC method in its traditional form is widely used and is well documented in literature, e.g. in a classical book by Bird (1994). Briefly, the region of the flow (e.g. plume expansion in laser ablation) is divided into a number of cells with the cell size determined by the local mean free path. The flow field is reproduced using a large number of simulated particles (typically  $10^6 - 10^7$ ) that are characterized by coordinates, velocities, internal energies, species type (radicals, ions, clusters of different sizes, etc.) and weight factor. The weight factor is defined by the number of real particles/species that are represented by each simulated particle. The evolution of the system of particles is split into collisionless streaming and collisions. At each time step all the particles are moved as if they do not interact, according to their current velocities and the external forces, e.g. gravitation or electric field force acting on ionized species. After all the particles are moved, a given number of particles are selected for collisions. Collision pairs are selected at random from the same cell regardless of the positions of the particles. New velocities are calculated as a result of each collision event. The collision frequency is defined by the relative velocities and the collision cross sections of the particles.

A fine grid of small black points in Part D of Figure 1 schematically represents the spatial resolution in the DSMC simulation. The kinetics of cluster evaporation/growth is reproduced by solving a system of rate equations, shown schematically by green squares. The latter provides input for DSMC calculations that take into account the change in the relative fractions of plume components. The coarse grid and the squares represent MD simulations of cluster-cluster and cluster-monomer collisions that are subsequently incorporated into DSMC simulation. The initial conditions for DSMC simulation are provided by MD simulations, as shown by the arrow in Figure 1. In order to make a connection be-

tween the MD simulation of laser ablation and the DSMC simulation of the ablation plume expansion, an appropriate description of a multi-component (containing a large number of clusters of different sizes) ablation plume obtained by the end of the MD simulation has to be developed [Zhigilei 2001, 2002]. The number of clusters of any given size observed in a MD simulation is not sufficient to provide a statistically adequate representation of the spatial distribution of clusters in the plume (except for the smallest clusters composed of up to 6-7 atoms/molecules). One possible solution to this problem is to divide clusters into groups. The range of cluster sizes that form a group can be chosen so that clusters in a group have similar velocity and spatial distributions in the plume. The characteristics that can provide a connection between MD and DSMC simulations in the multiscale model are summarized in Figure 3. First simulations performed with the combined MD-DSMC approach have demonstrated the ability of the method to provide insights into the complex processes occurring during the evolution of the ablation plume [Zeifman et al. 2002a, 2002b].

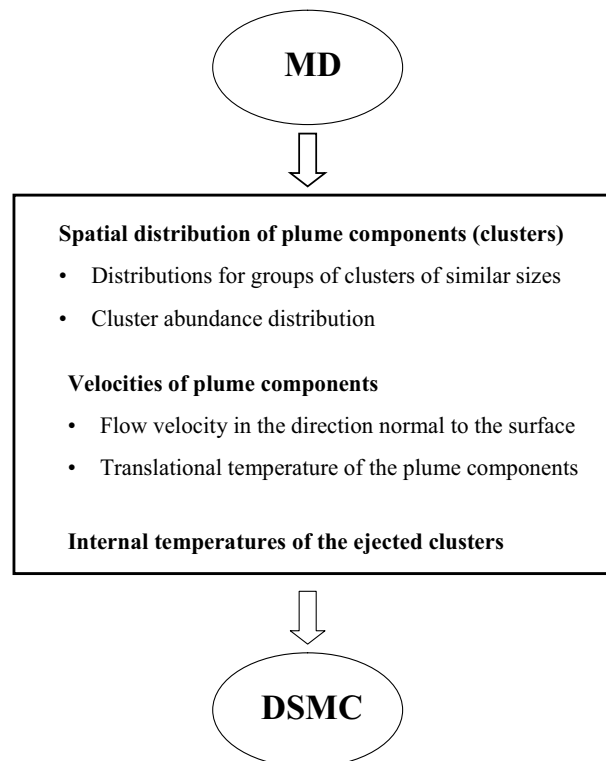


**Figure 3** : Connection between MD and DSMC

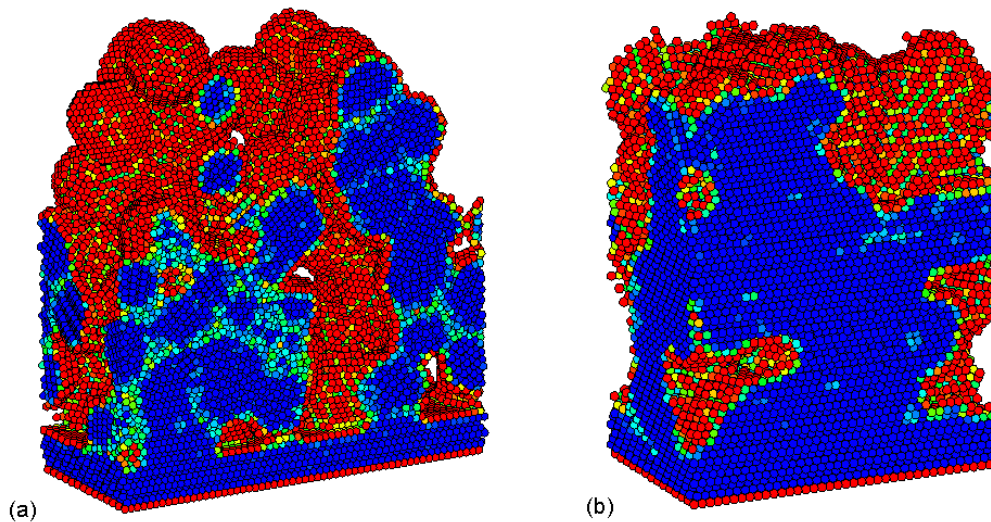


**Figure 4** : Atomic structure of films generated in MD simulations of Ni cluster deposition with impact velocities of (a) 1000 m/s and (b) 2000 m/s. The color corresponds to the potential energy of the atoms, from high potential energies of the surface atoms (red) to low potential energy of atoms in the bulk of a crystal (blue) [Dongare et al. 2001].

### 2.5 Film growth by cluster deposition

Multiscale simulations briefly outlined above can provide information on the cluster formation mechanisms and the effect of experimental conditions (irradiation parameters, type of the target material, background pressure and type of the background gas, length of the flight path, etc.) on the velocity and size distributions of clusters. Simulation results on the cluster formation in the ablation plume can provide a reliable input for computational investigation of the film deposition process, Part E of Figure 1. Clusters generated in laser ablation can be used to produce ultrafine powders, nanocomposites, and other nanostructured materials.

Molecular dynamics simulation technique has been demonstrated to be capable of providing insights into the mechanisms of film growth and the relation between the microscopic structure of the deposited films and parameters of the clusters [Cheng and Landman 1994; Hou et al. 2000; Kang et al. 2001]. Depending on the sizes of the deposited clusters and their initial kinetic energies, a variety of impact-induced assembly mechanisms can occur, including partial or complete epitaxy with the substrate, formation of extended defect structures, local melting and recrystallization. The morphology, porosity, texture, and the defect structures of the growing films are in a big part defined by the character of the fast processes

induced by the cluster impact events. For example, the effect of the impact energy on the morphology of a film growing by deposition of nickel clusters of 3 nm in diameter is apparent in Figure 4. This figure shows the results of MD simulations for two impact velocities, 1000 m/s and 2000 m/s. The initial cluster position and orientation relatively to the substrate are chosen at random for each deposited cluster. The temperature of the bulk region of the substrate is kept at 300 K during the simulation and intervals of 100 ps are kept between depositions of individual clusters to ensure complete dissipation of the deposited cluster energy and completion of the active relaxation processes induced by each impact. A mere visual inspection of the deposited films reveals the difference in the film microstructure. The film grown by the deposition of the lower-energy clusters has a lower density ( $\sim 75\%$  relative to the density of the substrate) and a complex nanostructure with voids of different sizes and large areas of internal surfaces and interfaces, Figure 4a. Only partial epitaxy to the substrate is observed in the first layer of clusters deposited, with random orientation of the crystallites located farther from the original substrate. The film produced at higher impact energies has higher density ( $\sim 90\%$  relative to the density of the substrate) and nearly perfect epitaxy to the substrate, Figure 4b. However, a relatively small number of voids is still formed during the growth process and a few stacking faults are



also present in the epitaxial layer. The observed difference in the structure of the growing films is the reflection of the difference in the impact-induced processes. In the case of the lower incident energy only a partial transient melting of a small contact region between the incoming cluster and the film takes place and clusters largely retain their crystal structure and orientation. The voids that are formed by the random cluster deposition do not collapse upon further cluster impacts. On the contrary, the higher-energy impact (2000 m/s) leads to the complete melting and recrystallization of the whole cluster and a large region of the film, leading to the epitaxial growth, smaller number of voids, and a higher overall density of the growing film.

Investigations of cluster deposition performed for a fixed cluster size and impact energy can provide some insight into the mechanisms of cluster deposition film growth. In real experiments, however, we typically have a range of impact velocities and a range of cluster sizes deposited. An important advantage of the multiscale computational approach discussed in this paper for laser ablation cluster generation and deposition, is that it allows us to directly relate the parameters of deposited clusters to the laser irradiation conditions. Sizes, velocities, internal temperatures of the clusters can be obtained from the combined MD - DSMC simulations, as discussed above.

### **3 Generation of nanoparticles in laser ablation: MD simulation**

MD method has been demonstrated to be capable of providing detailed information on the mechanisms of cluster formation in laser ablation, parameters of the ejected clusters, and their dependence on the irradiation conditions [Zhigilei and Garrison 2000; Zhidkov et al. 2001; Zhigilei 2002]. For example, snapshots from MD simulations of laser ablation of a molecular solid performed at different laser fluences and pulse widths, shown in Figure 5, illustrate several mechanisms of cluster formation in laser ablation. At sufficiently high laser fluences, the phase explosion of the overheated material leads to the formation of a foamy transient structure of interconnected liquid regions that subsequently decomposes into a mixture of liquid droplets, gas-phase molecules, and small clusters, Figure 5a. The ejection of large droplets at lower laser fluences can be attributed to the transient melting and hydrodynamic motion of the liquid caused by steep thermal gradients and relaxation of the laser-

induced pressure in the vicinity of the melted surface, Figure 5b. The ejection of large fractured solid fragments can be caused by photomechanical effects driven by the relaxation of the laser induced stresses, Figure 5c. The magnitude of the laser induced stresses and the role of the associated photomechanical effects in material ejection become significant under conditions of stress confinement, when the laser pulse duration is shorter than the time needed for mechanical equilibration of the absorbing volume [Oraevsky et al. 1995; Itzkan 1995; Zhigilei and Garrison 2000].

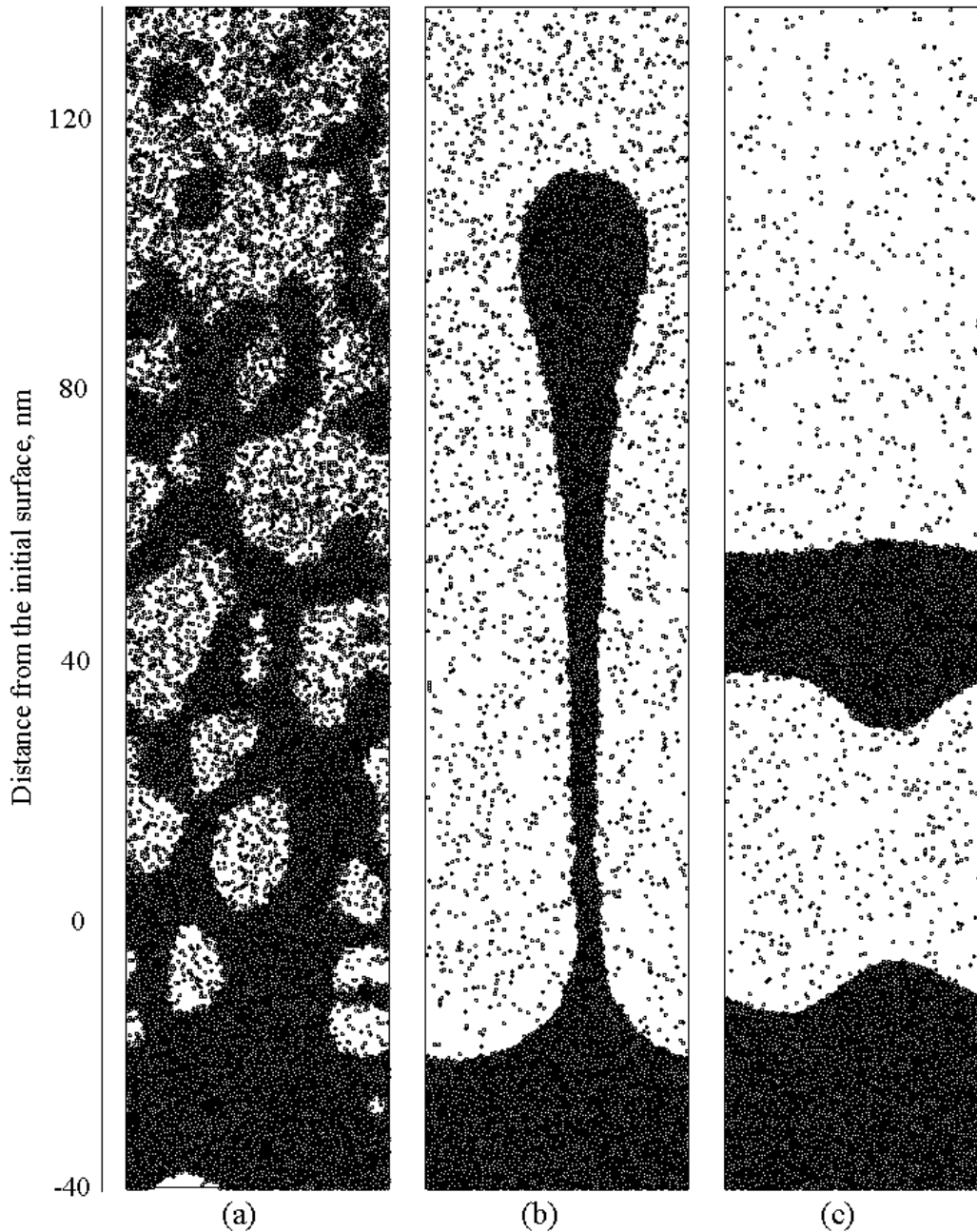


**Figure 5** : Snapshots from MD simulations of laser ablation of a molecular solid illustrating different mechanisms of cluster ejection: (a) phase explosion of the overheated material; (b) hydrodynamic sputtering due to a transient melting and motion of the liquid in the surface region; (c) photomechanical spallation of the surface layer caused by the relaxation of laser-induced thermoelastic stresses.

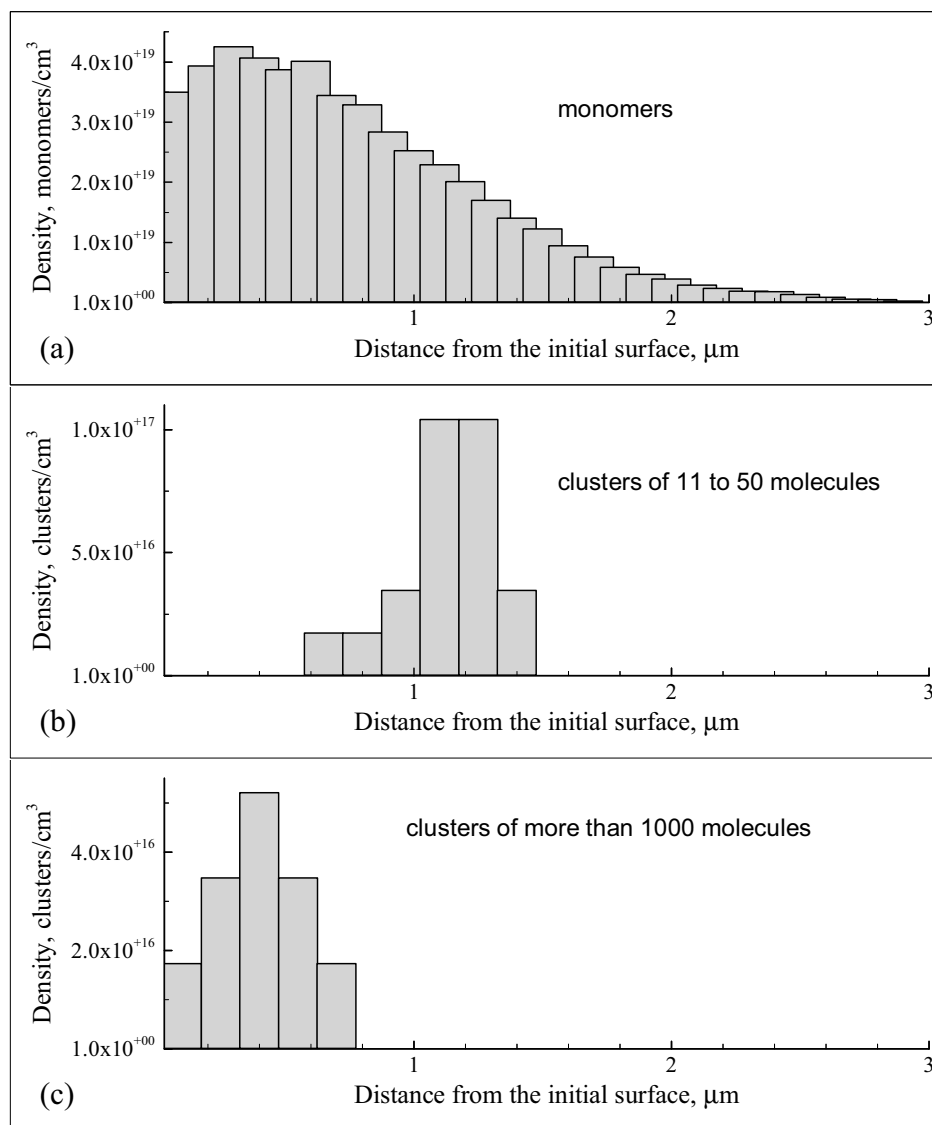


**Figure 6** : Number density of clusters of different sizes in the ablation plume as a function of the distance from the initial surface. The data is shown for 1 ns after irradiation of a molecular soled with a 15 ps laser pulse at laser fluence of  $61 \text{ J/m}^2$ .

At sufficiently high laser fluences, laser ablation results in the ejection of clusters of a wide range of sizes, e.g. Figure 5a. Spatially-resolved analysis of the ablation plume performed at the end of the MD simulation, when the process of the formation of well-defined spherical droplets in the plume is complete, reveals the effect of segregation of the clusters of different sizes in the expanding plume [Zhigilei 2001, 2002]. The largest clusters are formed in the region closest to the surface, medium-size clusters are formed in the middle of the plume, and small clusters are formed in the top part of the plume, with almost no regions of coexistence of clusters of different sizes. Three example distributions, for individual molecules, for medium-size molecular clusters (11 to 50 molecules), and for large molecular clusters composed of more than 1000 molecules are shown in Figure 6 for a simulation performed with 15 ps laser pulse and laser fluence 2.1 times the threshold fluence for the onset of the massive material ejection or ablation. The distribution for monomers follows the prediction of the free expansion model with somewhat reduced density near the surface of the target due to the redeposition of molecules to the target. The medium size clusters are localized in the middle of the expanding plume, whereas the large clusters formed later during the plume development tend to be slower and are closer to the original surface. Spatial segregation of the ejected clusters in the plume provides opportunities for cluster separation (by a mechanical chopper or other means [e.g. Chrisey and Hubler 1994; Knowles and Leone 1997]) and deposition of mass-selected clusters in film growth.

The abundance distributions of the ejected clusters are shown in Figure 7 for the same simulation discussed above. In the cluster distribution, plotted in double-logarithmic scale, one can readily distinguish two distinct regions that correspond to small, up to  $\sim 15$  molecules, and large clusters. The cluster size distributions can be relatively well described by a power law  $Y(N) \sim N^{-\tau}$  with exponents different for the low- and high-mass clusters. The decay is much slower in the high mass region of the distribution – the exponent  $-\tau$  is 2-3 times larger. A power law for cluster yield distribution has been predicted for the gas-liquid phase transition occurring at the critical point [Urbassek 1988] and for self-similar fragmentation processes [Bershadskii 2000]. It has also been commonly observed in sputtering experiments [Colla et al. 1998; Hamza et al. 1999] and MD simulations

[Wucher and Garrison 1996; Colla et al. 1998; Muramoto et al. 2001]. However, the complex character of laser ablation process makes it difficult to establish a direct link between any of the existing theoretical models and the results of the present simulations. Qualitatively, the existence of the two, low- and high-mass, regions in the cluster abundance distributions can be related to the processes leading to the ablation plume formation, discussed above. The monomers and small clusters are released in the explosive decomposition of the overheated material into the liquid and vapor, whereas the larger clusters appear as a result of decomposition and coarsening of the transient liquid structure of interconnected liquid regions. In addition to the spatial and abundance distributions described above, MD simulations provide complete information on the plume composition and velocities of different plume components [Zhigilei and Garrison 2000; Zhigilei 2001, 2002] that can be adapted as input for DSMC simulations, Figures 1 and 3.

#### 4 Molecular implantation/deposition by nano-jet ejection from a micropipette

Another application of laser ablation in nanotechnology, that has been investigated using MD simulation technique, is a new method for controlled transfer of organic molecules to designated regions of a polymer substrate [Goto et al. 1999, 2000, 2001]. In this technique, laser irradiation of a microscopic amount of molecular substance spatially confined in the tip of a glass nanopipette having aperture of 100 nm is used to create sub-micron implanted fluorescent features or deposit clusters of molecules on a polymer substrate. Experimental investigation of this technique has revealed a strong fluence dependence of the molecular ejection process and hence the final distribution of the deposited molecules. Three distinct regimes have been identified. At laser fluences below certain threshold fluence no implantation or molecular transfer to the substrate is observed. Just above the threshold fluence, formation of a well-defined molecular cluster at the surface of the polymer substrate has been observed. No implantation into the polymer substrate is observed in this regime and the cluster can be moved around the substrate with an AFM tip. At higher laser fluences an efficient implantation of the ejected molecules into a sub-micron region of the substrate is observed.

In order to get a qualitative understanding of the pro-

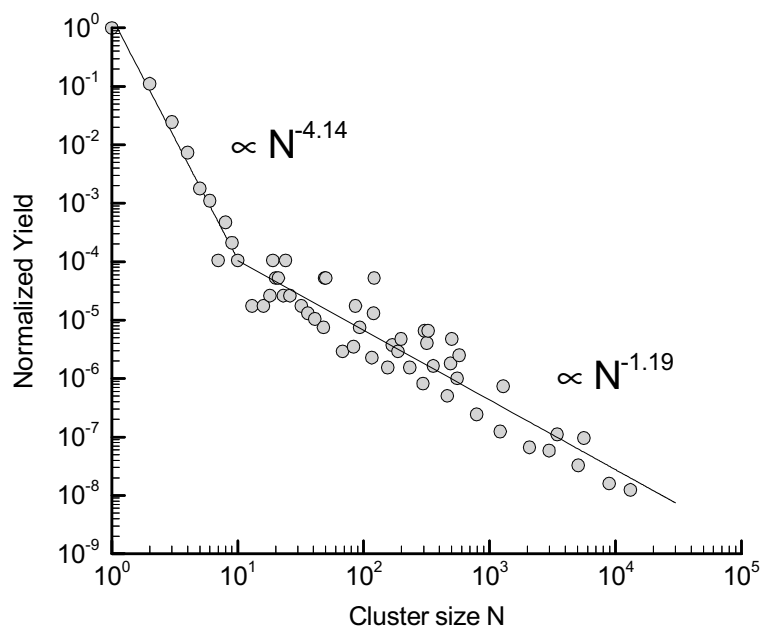


**Figure 7** : Cluster abundance distribution in the ablation plume at 1 ns after irradiation of a molecular solid with 15 ps laser pulse at laser fluence of  $61 \text{ J/m}^2$ .

cesses leading to the implantation or cluster deposition, a series of simulations of molecular ejection from a doped nano-pipette has been performed [Goto et al. 2001]. The simulations were performed using the breathing sphere model [Zhigilei et al. 1997, 1998] that was adapted to match the experimental system. The snapshots from the simulations at three different laser fluences are shown in Figure 8. A visual inspection of the snapshots reveals a strong fluence dependence of the molecular ejection process. At low laser fluences molecular material melts inside the tip, a small number of molecules is ejected, but no molecular transfer to the substrate occurs, Figure 8a. As fluence increases, the temperature of the molecular material in the tip increases above the boiling point leading to the release of the gas phase molecules and expulsion of a liquid droplet from the tip, Figure 8b. In this simulation the bulk part of the ejected liquid is deposited to the substrate, cools down due to the evaporation and heat conduction to the substrate, and forms of a compact nanocluster similar to the ones observed experimentally at sub-implantation fluences. An additional increase of laser fluence leads to a stronger overheating and explosive boiling of the molecular material in the pipette tip. A hot mixture of gas-phase molecules and small clusters is ejected from the tip at these high fluences, Figure 8c. The high temperature of the ejected material and the

high ejection velocities (up to 1000 m/s in the front of the ejecta) can lead to the transient melting of the exposed polymer surface region and efficient implantation of the ejected molecules into the substrate, as observed in experiments at high laser fluences.

#### 4.1 Summary

As the range of applications of laser ablation phenomenon in the area of nanotechnology is quickly expanding, the computational modeling of laser-induced processes at the atomic/molecular level has a potential of making an important contribution to the optimization of existing applications and the development of new ideas and approaches. In order to realize this potential, several challenging computational problems have to be addressed. In particular, an adequate description of the laser light coupling to a target material and different channels of relaxation of the primary elementary excitations has to be developed and incorporated into conventional simulation techniques. Different computational approaches have to be developed for different types of materials and different irradiation conditions. Moreover, the laser ablation is a complex multiscale phenomenon that involves processes occurring at different time and length scales and cannot be described within a single computational model.

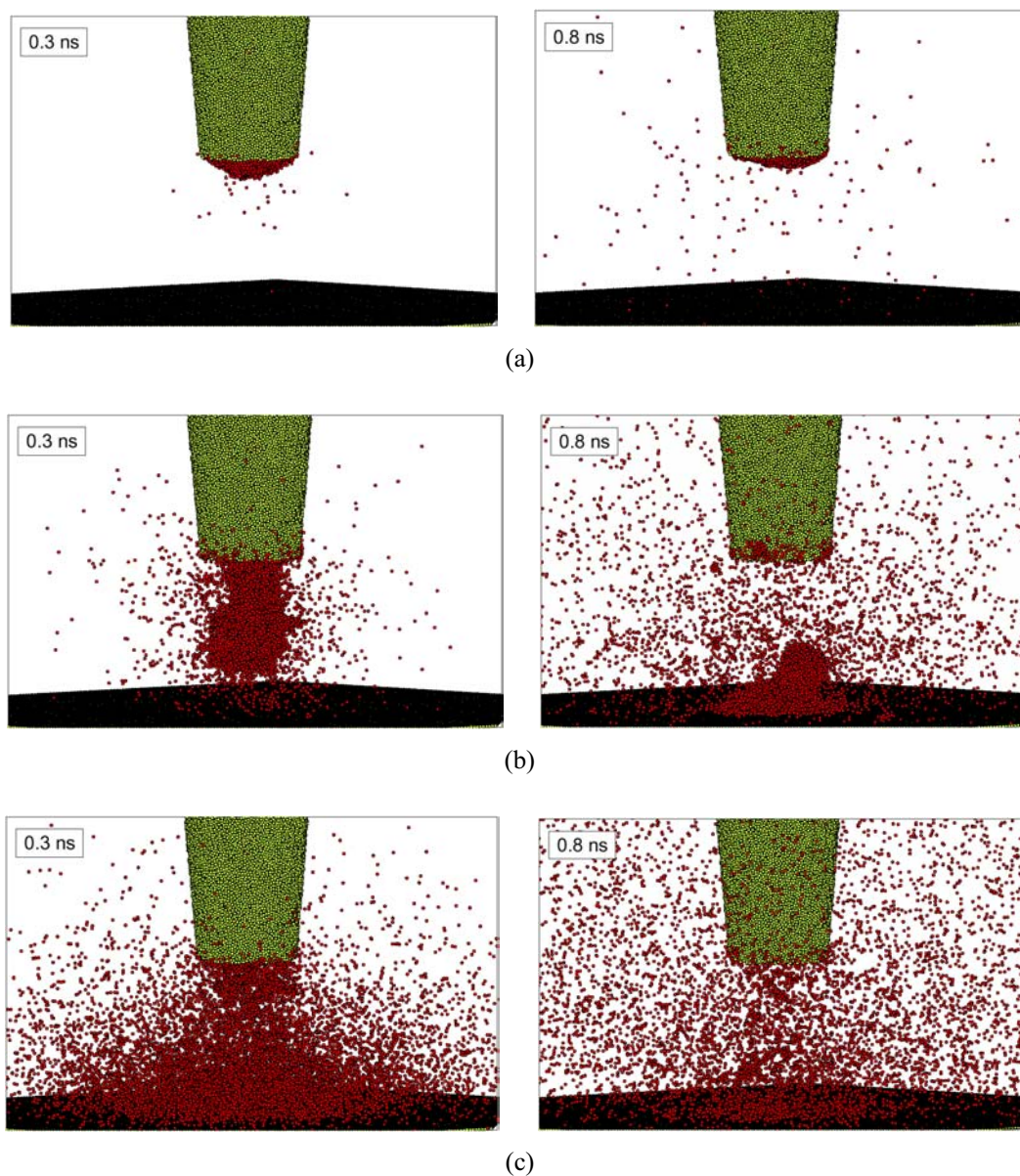


**Figure 8** : Snapshots from the simulations of molecular ejection from an irradiated pipette tip. The laser pulse duration is 100 ps, the energy densities deposited by the laser pulse are (a) 0.2 eV/molecule, (b) 0.4 eV/molecule, (c) 0.8 eV/molecule.

In this paper we discuss two computational schemes developed for simulation of laser coupling to organic materials and metals and present a multiscale model for laser ablation and cluster deposition of nanostructured materials. In the multiscale model the initial stage of laser ablation is reproduced by the MD breathing sphere model in the case of organic materials or by an atomistic MD method combined with the two-temperature model in the case of metals. The two temperature model coupled to the MD model provides an adequate description of the laser energy absorption into the electronic system and fast electron heat conduction in metals. A combined molecular dynamics - finite element method or the dynamic boundary condition is used to avoid reflection of the laser-induced pressure wave from the boundary of the MD computational cell. The direct simulation Monte Carlo method is used for simulation of the long term ablation plume expansion, and the MD method is used to simulate film growth by cluster deposition from the ablation plume.

The proposed multiscale approach has been shown to be capable of providing information on the mechanisms of cluster formation in laser ablation as well as on the distribution of clusters of different sizes in the ejected plume. The parameters of the ejected ablation plume can be used in simulations of film growth by cluster deposition, allowing us to directly relate the parameters of the deposited clusters to the laser irradiation conditions. First MD simulations of cluster deposition have revealed a strong dependence of the structure of the growing films on the parameters of the deposited clusters.

The effect of spatial confinement in laser ablation, utilized in a new laser-enabled technique for nano-scale molecular transfer, has been investigated by molecular-level modeling. In this case a controlled deposition of organic molecules into a polymer substrate is achieved by laser irradiation of a microscopic amount of molecular substance confined in the tip of a micropipette. This method allows for a fine spatial control in implantation of functional organic molecules into a designated region of an organic substrate and has potential applications in bio- and nano-technology.

**Acknowledgement:** Financial support of this work was provided by the National Science Foundation through the Materials Research Science and Engineering Center for Nanoscopic Materials Design at the Univer-

sity of Virginia by the University of Virginia through the new faculty start-up funds, and by the Air Force Office of Scientific Research through the Medical Free Electron Laser Program. Partial computational support was provided by the National Partnership for Advanced Computational Infrastructure (NPACI) program. The authors would like to thank Patrick Lorazo for insightful comments and suggestions.

## References

- Anisimov, S.I.; Kapeliovich, B.L.; Perel'man, T.L.** (1974): Electron emission from metal surfaces exposed to ultrashort laser pulses. *Sov. Phys. JETP*, vol. 39, pp. 375-377.
- Ayyub, P.; Chandra, R.; Taneja, P.; Sharma, A.K.; Pinto, R.** (2001): Synthesis of nanocrystalline material by sputtering and laser ablation at low temperatures. *Appl. Phys. A*, vol. 73, pp. 67-73.
- Bäuerle, D.** (2000): *Laser processing and chemistry*, Springer-Verlag, Berlin Heidelberg.
- Bershadskii, A.** (2000): Multiscaling and localized instabilities in fracture, fragmentation, and growth processes. *Eur. Phys. J. B*, vol. 14, pp. 323-327.
- Bird, G.A.** (1994): *Molecular gas dynamics and the direct simulation of gas flows*, Clarendon Press, Oxford.
- Birdsall, C.K.** (1991): Particle-in-cell charged-particle simulations, plus Monte Carlo collisions with neutral atoms, PIC-MCC. *IEEE Trans. Plasma Sci.*, vol. 19, pp. 65-85.
- Chen, H.-P.; Landman, U.** (1994): Controlled deposition and glassification of copper nanoclusters. *J. Phys. Chem.*, vol. 98, pp. 3527-3537.
- Chrissey, D.B.; Hubler, G.K.** (eds) (1994): *Pulsed laser deposition of thin films*, Wiley-Interscience, New York.
- Colla, Th.J.; Urbassek, H.M.; Wucher, A.; Staudt, C.; Heinrich, R.; Garrison, B.J.; Dandachi, C.; Betz, G.** (1998): Experiment and simulation of cluster emission from 5keV Ar  $\rightarrow$  Cu. *Nucl. Instrum. Meth. Phys. Res. B*, vol. 143, pp. 284-297.
- Daw, M.S.; Foiles, S.M.; Baskes, M.I.** (1993): The embedded-atom method: a review of theory and applications. *Mat. Sci. Rep.*, vol. 9, pp. 251-310.
- Deák, J.C.; Iwaki, L.K.; Rhea, S.T.; Dlott, D.D.** (2000): Ultrafast infrared-Raman studies of vibrational energy redistribution in polyatomic liquids. *J. Raman Spectr.*, vol. 31, pp. 263-274.

- Dekel, E.; Eliezer, S.; Henis, Z.; Moshe, E.; Ludmirsky, A.; Goldberg, I.B.** (1998): Spallation model for the high strain rates range. *J. Appl. Phys.*, vol. 84, pp. 4851-4858.
- Dongare, M.A.; Hass, D.D.; Zhigilei, L.V.** (2001): Molecular dynamics simulations of cluster deposition film growth. Unpublished results.
- Fitz-Gerald, J.; Pennycook, S.; Gao, H.; Singh, R.K.** (1999): Synthesis and properties of nanofunctionalized particulate materials. *Nanostruct. Mater.*, vol. 12, pp. 1167-1171.
- Goto, M.; Hobley, J.; Kawanishi, S.; Fukumura, H.** (1999): Laser-induced implantation of organic molecules into sub-micrometer regions of polymer surfaces. *Appl. Phys. A*, vol. 69, pp. S257-S261.
- Goto, M.; Kawanishi, S.; Fukumura, H.** (2000): Laser implantation of dicyanoanthracene in poly(methyl methacrylate) from a 100-nm aperture micropipette. *Appl. Surf. Sci.*, vol. 154-155, pp. 701-705.
- Goto, M.; Zhigilei, L. V.; Hobley, J.; Kishimoto, M.; Garrison, B. J.; Fukumura, H.** (2001): Laser expulsion of an organic molecular nano-jet from a confined domain onto a polymer surface. *J. Appl. Phys.*, vol. 90, pp. 4755-4760.
- Häkkinen, H.; Landman, U.** (1993) Superheating, melting, and annealing of copper surfaces. *Phys. Rev. Lett.*, vol. 71, pp. 1023-1026.
- Hamza, A.V.; Schenkel, T.; Barnes, A.V.** (1999): Dependence of cluster ion emission from uranium oxide surfaces on the charge state of the incident slow highly charged ion. *Eur. Phys. J. D*, vol. 6, pp. 83-87.
- Hillenkamp, F.; Karas, M.** (2000): Matrix-assisted laser desorption/ionization, an experience. *Int. J. Mass Spectrom.*, vol. 200, pp. 71-77.
- Hou, Q.; Hou, M.; Bardotti, L.; Prevel, B.; Melinon, P.; Perez, A.** (2000): Deposition of Au<sub>N</sub> clusters on Au(111) surfaces. I. Atomic-scale modeling. *Phys. Rev. B*, vol. 62, pp. 2825-2834.
- Itina, T.E.; Zhigilei, L.V.; Garrison, B.J.** (2002): Microscopic mechanisms of matrix assisted laser desorption of analyte molecules: Insights from molecular dynamics simulation. *J. Phys. Chem. B*, vol. 106, pp. 303-310.
- Itzkan, I.; Albagli, D.; Dark, M.L.; Perelman, L.T.; von Rosenberg, C.; Feld, M.S.** (1995): The thermoelastic basis of short pulsed laser ablation of biological tissue. *Proc. Natl. Acad. Sci. USA*, vol. 92, pp. 1960-1964.
- Ivanov, D.S.; Zhigilei, L.V.** (2002): Microscopic analysis of ultrafast laser melting of thin metal films. (In Preparation)
- Jersch, J.; Demming, F.; Hildenhagen, J.; Dickmann, K.** (1997): Nano-material processing with laser radiation in the near field of a scanning probe tip. *Opt. Laser Technol.*, vol. 29, pp. 433-437.
- Kang, J.W.; Choi, K.S.; Kang, J.C.; Kang, E.S.; Byun, K.R.; Hwang, H.J.** (2001): Cluster deposition study by molecular dynamics simulation: Al and Cu cluster. *J. Vac. Sci. Technol. A*, vol. 19, pp. 1902-1906.
- Kim, H.; Dlott, D.** (1991): Molecular dynamics simulation of nanoscale thermal conduction and vibrational cooling in a crystalline naphthalene cluster. *J. Chem. Phys.*, vol. 94, pp. 8203-8209.
- Knowles, M.P.; Leone, S.R.** (1997): Generation of velocity selected, pulsed source of hyperthermal (1-10 eV) neutral metal atoms for thin film growth studies. *J. Vac. Sci. Technol. A*, vol. 15, pp. 2709-2716.
- Lorazo, P.; Lewis, L.J.; Meunier, M.** (2000): Picosecond pulsed laser ablation of silicon: a molecular-dynamics study. *Appl. Surf. Sci.*, vol. 168, pp. 276-279.
- Miotello, A.; Kelly, R.** (1999): Laser-induced phase explosion: new physical problems when a condensed phase approaches the thermodynamic critical temperature. *Appl. Phys. A*, vol. 69, pp. S67-S73.
- Muramoto, T.; Okai, M.; Yamashita, Y.; Yorizane, K.; Yamamura, Y.** (2001): MD simulation of cluster formation during sputtering. *Nucl. Instrum. Meth. Phys. Res. B*, vol. 180, pp. 222-229.
- Niemz, M.H.** (1996): *Laser-tissue interactions: fundamentals and applications*, Springer-Verlag, Berlin Heidelberg.
- Ohmura, E.; Fukumoto, I.** (1996): Molecular dynamics simulation on laser ablation of fcc metal. *Int. J. Japan Soc. Prec. Eng.*, vol. 30, pp. 128-133.
- Ohmura, E.; Fukumoto, I.** (1997): Modified molecular dynamics simulation on laser ablation of metal. *Int. J. Japan Soc. Prec. Eng.*, vol. 31, pp. 206-207.
- Oraevsky, A.A.; Jacques, S.L.; Tittel, F.K.** (1995): Mechanism of laser ablation for aqueous media irradiated under confined-stress conditions. *J. Appl. Phys.*, vol. 78, pp. 1281-1290.
- Oran, E. S.; Oh, C. K.; Cybyk, B. Z.** (1998): Direct



- simulation Monte Carlo: recent advances and applications, *Annu. Rev. Fluid Mech.*, vol. 30, pp. 403-441.
- Puretzky, A.A.; Geohegan, D.B.; Fan, X.; Pennycook, S.J.** (2000): Dynamics of single-wall carbon nanotube synthesis by laser vaporization. *Appl. Phys. A*, vol. 70, pp. 153-160.
- Rudd, R.E.; Broughton, J.Q.** (2000): Concurrent coupling of length scales in solid state systems. *Phys. Status Solidi B*, vol. 217, pp. 251-291.
- Schäfer, C.; Urbassek, H.M.; Zhigilei, L.V.; Garrison, B.J.** (2002a): Pressure-transmitting boundary conditions for molecular dynamics simulations. *Comp. Mater. Sci.*, vol. 24, pp. 421-429.
- Schäfer, C.; Urbassek, H.M.; Zhigilei, L.V.** (2002b): Metal ablation by picosecond laser pulses: A hybrid simulation. *Phys. Rev. B*, in press.
- Smirnova, J.A.; Zhigilei, L.V.; Garrison, B.J.** (1999): A combined molecular dynamics and finite element method technique applied to laser induced pressure wave propagation. *Comput. Phys. Commun.*, vol. 118, pp. 11-16.
- Urbassek, H.M.** (1988): Sputtered cluster mass distributions, thermodynamic equilibrium, and critical phenomena. *Nucl. Instrum. Meth. Phys. Res. B*, vol. 31, pp. 541-550.
- Williams, G.J.; Zhigilei, L.V.; Garrison, B.J.** (2001): Laser ablation in a model two-phase system. *Nucl. Instr. Meth. B*, vol. 180, pp. 209-215.
- Wucher, A.; Garrison, B.J.** (1996): Cluster formation in sputtering: A molecular dynamics study using the MD/MC-corrected effective medium potential. *J. Chem. Phys.*, vol. 105, pp. 5999-6007.
- Yingling, Y.G.; Zhigilei, L.V.; Garrison, B.J.** (2001): The role of photochemical fragmentation in laser ablation: A molecular dynamics study. *J. Photochem. Photobiol. A*, vol. 145, pp. 173-181.
- Zeifman, M.I.; Garrison, B.J.; Zhigilei, L.V.** (2002a): Direct simulation Monte Carlo calculation: strategies for using complex initial conditions. *Mat. Res. Soc. Symp. Proc.*, vol. 731, pp. W3.8.1-W3.8.6.
- Zeifman, M.I.; Garrison, B.J.; Zhigilei, L.V.** (2002b): Combined molecular dynamics – direct simulation Monte Carlo computational study of laser ablation plume evolution, *J. Appl. Phys.*, vol. 92, in press.
- Zhang, Y.F.; Tang, Y.H.; Wang, N.; Yu, D.P.; Lee, C.S.; Bello, I.; Lee, S.T.** (1998): Silicon nanowires prepared by laser ablation at high temperature. *Appl. Phys. Lett.*, vol. 72, pp. 1835-1837.
- Zhidkov, A.G.; Sasaki, A.** (1998): Hybrid particle-in-cell (PIC) simulation of heat transfer and ionization balance in overdense plasmas irradiated by sub-picosecond pulse lasers. *JAERI-Research 98-068 report*, Japan Atomic Energy Research Institute.
- Zhidkov, A.G.; Zhigilei, L.V.; Sasaki, A.; Tajima, T.** (2001): Short-laser-pulse driven emission of energetic ions into a solid target from a surface layer spalled by a laser prepulse. *Appl. Phys. A*, vol. 73, pp. 741-747.
- Zhigilei, L.V.; Kodali, P.B.S.; Garrison, B.J.** (1997): Molecular dynamics model for laser ablation of organic solids. *J. Phys. Chem. B*, vol. 101, pp. 2028-2037.
- Zhigilei, L.V.; Kodali, P.B.S.; Garrison, B.J.** (1998): A microscopic view of laser ablation. *J. Phys. Chem. B*, vol. 102, pp. 2845-2853.
- Zhigilei, L.V.; Garrison, B.J.** (1998): Microscopic simulation of short pulse laser damage of melanin particles. In: S. L. Jacques (ed) *Laser-tissue interaction IX*, (Proc. SPIE, vol. 3254) pp. 135-143.
- Zhigilei, L.V.; Garrison, B.J.** (1999): Pressure waves in microscopic simulations of laser ablation. In: T. Diaz de la Rubia, T. Kaxiras, V. Bulatov, N.M.Ghoniem, R. Phillips (eds) *Multiscale modelling of materials* (Mat. Res. Soc. Symp. Proc., vol. 538) pp. 491-496.
- Zhigilei, L.V.; Garrison, B.J.** (2000): Microscopic mechanisms of laser ablation of organic solids in the thermal and stress confinement irradiation regimes. *J. Appl. Phys.*, vol. 88, pp. 1281-1298.
- Zhigilei, L.V.** (2001): Computational model for multi-scale simulation of laser ablation. In: V.V. Bulatov, F. Cleri, L. Colombo, L.J. Lewis, N. Mousseau (eds) *Advances in materials theory and modeling - bridging over multiple length and time scales* (Mat. Res. Soc. Symp. Proc., vol. 677), pp. AA2.1.1-AA2.1.11.
- Zhigilei, L.V.** (2002): Dynamics of the plume formation and parameters of the ejected clusters in short-pulse laser ablation. *Appl. Phys. A*, in press.

